J Mater Sci: Mater Med (2009) 20:2527–2540
DOI 10.1007/s10856-009-3818-x

Preparation, characterization and in vitro biological study of biomimetic three-dimensional gelatin–montmorillonite/cellulose scaffold for tissue engineering

Ahmed A. Haroun · Amira Gamal-Eldeen · David R. K. Harding

Received: 5 February 2009 / Accepted: 1 July 2009 / Published online: 23 July 2009

Abstract This work focused on studying the effect of blending gelatin (Gel) with Cellulose (Cel), in the presence of montmorillonite (MMT), on the swelling behavior, in vitro degradation and surface morphology. Additionally, the effect of the prepared biocomposites on the characteristics of the human osteosarcoma cells (Saos-2), including proliferation, scaffold/cells interactions, apoptosis and their potential of the cells to induce osteogenesis and differentiation was evaluated. The crosslinked biocomposites with glutaraldehyde (GA) or *N,N*-methylene-bisacrylamide (MBA) was prepared via an intercalation process and freeze-drying technique. Properties including SEM morphology, X-ray diffraction characterization and in vitro biodegradation were investigated. The successful generation of 3-D biomimetic porous scaffolds incorporating Saos-2 cells indicated their potential for de novo bone formation that exploits cell–matrix interactions. In vitro studies revealed that the scaffolds containing 12 and 6% MMT crosslinked by 5 and 0.5% GA seem to be the two most efficient and effective biodegradable scaffolds, which promoted Saos-2 cells proliferation, migration, expansion, adhesion, penetration, spreading, and differentiation, respectively. MMT improved cytocompatibility between the osteoblasts and the biocomposite. In vitro analysis indicated good biocompatibility of the scaffold and presents the scaffold as a new potential candidate as suitable biohybrid material for tissue engineering.

A. A. Haroun (✉)
Chemical Industries Research Division, Center of Excellency for Advanced Sciences, National Research Centre, Dokki, 12622 Cairo, Egypt
e-mail: haroun68_2000@yahoo.com

A. Gamal-Eldeen
Cancer Biology Laboratory, Center of Excellency for Advanced Sciences, National Research Centre, Dokki, 12622 Cairo, Egypt

D. R. K. Harding
College of Science, Institute of Fundamental Sciences, Massey University, Palmerston North, New Zealand

1 Introduction

A suitable bio-acceptable scaffold is one of the key factors required for successful tissue engineering leading to tissue regeneration. Tissue engineering is a rapidly developing area that requires the use of biodegradable and biocompatible scaffolds as three-dimensional supports for initial cell attachment and subsequent tissue organization, formation and growth [1]. A variety of porous materials have been used to produce three-dimensional composites for cell growth. These composites are designed to allow individual cells to attach to the scaffold surface while promoting cell growth and maintaining the differentiated cell phenotypes [2, 3]. For a tissue to be successfully regenerated, sufficient cell propagation and appropriate differentiation must be achieved in the three-dimensional cellular composite. Nonwoven fabrics are widely used as scaffolds for tissue engineering application [4]. The polysaccharide scaffolds are usually prepared by a freeze-drying methodology [5]. Gelatin (Gel), the denatured derivative of collagen, is a biocompatible protein that exhibits low antigenicity and very high bio-absorptivity in vivo. It can be used as a scaffold for tissue engineering and the efficacy of crosslinked Gel-based sponges composed of Gel and polysaccharides for wound-dressing materials had been reported [6, 7]. Gel can be obtained from inexpensive sources such as wastes and by-products generated in different manufacturing processes such as the tanning, pharmaceutical and food processing industries [8]. The three-dimensional gel

network of Gel is composed of microcrystalline segments interconnected with amorphous regions of randomly coiled segments [9, 10]. Gel has been recently used as a scaffold for cartilage tissue engineering, because it is not immunogenic compared to its precursor, and can promote cell adhesion, migration, differentiation, and proliferation [11, 12]. The authors attached the tripeptide, arginine–glycine–aspartic acid, to the composite to promote cell adhesion and migration in addition to forms a polyelectrolyte complex [13]. Montmorillonite (MMT) is a layered silicate [$Na_{0.7}$ ($Al_{3.3}$ $Mg_{0.7}$) Si_8 O_{20} $(OH)_4 \cdot nH_2O$] and known as polymer modifier due to its classical use as a filler and its high specific surface area (up to 600 m^2/g) [14]. Specific studies on the biocompatibility of natural polymers/MMT nanocomposites have rarely been reported [15]. However, synthetic polymers/MMT nanocomposites have received considerable attention [16–20]. Despite the attraction of these composites, the strength of the scaffolds is not good enough for hard tissue engineering. With only a low content of MMT, the mechanical properties and solvent resistance of composites can be greatly improved. As a bioinert clay mineral, MMT has been applied in the pharmaceutical industry for the preparation of porous biodegradable scaffolds for tissue engineering [21]. Cellulose (Cel) is a natural polymer consisting of D-anhydro-glucose ($C_6H_{11}O_5$) repeating unit joined by 1,4-β-D-glycosidic linkages at C_1 and C_4. Each repeating unit contains three hydroxyl groups. These hydroxyl groups, with their ability to form hydrogen bond, play a major role in directing the crystalline packing and also govern the physical properties of Cel. Solid Cel forms are comprised of microcrystalline regions and amorphous regions [22]. The pure microbial Cel membrane can accelerate the healing process of acute and chronic skin wounds. Thus, the medicinal properties of microbial Cel can be augmented when used with other polymers to form composites. In addition the composite scaffolds hold promise for tissue engineering to accelerate the healing process [23]. To our knowledge, the use of a Gel–MMT/Cel biocomposites as scaffolds for tissue regeneration has not been reported. This work focused on studying the effect of blending Gel with Cel, in the presence of MMT, on the swelling behavior, in vitro degradation and structure morphology. The 3-D scaffolds from various blend ratios were achieved using a controlled rate freezing and lyophilization technique. Additionally, the effect of the prepared biocomposites on the characteristics of the human osteosarcoma cells (Saos-2), including proliferation, scaffold/cells interactions, apoptosis and their potential of the cells to induce osteogenesis and differentiation was evaluated. Moreover, we screened the effect of biocomposites on the macrophages proliferation as a representative type of immune cells and checked their inflammatory effect using macrophages.

2 Materials and methods

2.1 Materials

Reagent grade chemicals were purchased from Sigma–Aldrich unless otherwise stated and were used without further purification. Gel from porcine skin, type A, was obtained from Sigma–Aldrich. Cel was obtained from Riedel De Haen AG, surface area about 5,500 cm^2 and fiber diameter (20–75 μm). Montmorillonite K_{10} was obtained from Fluka, pH 2.5–3.5, and particle size around 40 μm. Except where mentioned, all culture materials and all chemicals were obtained from Cambrex Bioscience, Copenhagen, Denmark and from Sigma, USA, respectively. Human osteogenic sarcoma (Saos-2) and Raw murine macrophage (RAW 264.7) was purchased from ATCC, VA, USA.

2.2 Preparation of Gel–MMT/Cel Biocomposites

MMT suspensions with different concentrations (6% and 12 w/v% in water) ultrasonically pretreated were added drop-wise into 6 wt% Gel solution at 70°C under agitation for 1 h. Then 6 wt% sterile Cel suspension (autoclaved at 121°C in a wet cycle for 20 min) was added to the above homogenous mixture at 40°C. After fast agitation for 4 h, the mixture was degassed with nitrogen. Then different concentrations of 25% glutaraldehyde (GA) solution (0.25, 0.5 and 1.0 v/v%) or 0.5% *N,N*-methylene-bisacrylamide (MBA) were added into the above mixtures and slowly stirred at 40°C for a further 1 h. The crosslinked products were poured into a Petri dish and frozen for 12 h at −80°C. Then the frozen samples were lyophilized within a freeze–dryer for 48 h. The porous scaffold obtained was treated with 0.5 g of cysteine to remove non-reacted aldehyde groups, rinsed with double distilled water and lyophilized again.

2.3 Biocomposite swelling studies

The swelling evaluation was previously carried out [24, 25]. Weighed dried samples were soaked in 10 ml of 0.05 M phosphate buffer saline (PBS) which was prepared with different pH values (2.0, 7.4 and 9.0) for 7 days at 37°C [26]. After the predetermined time, the scaffolds (gels) were withdrawn from the solution, surface dried with a clean paper and re-weighed. Then the swelling degree S_w (%) was calculated using the following equation:

$$S_w(\%) = [(W_w - W_d)/W_d] \times 100$$

where W_w and W_d are the wet and dry gel weight, respectively.

2.4 In vitro biodegradation

The in vitro biodegradation behavior of scaffolds was studied using the method of Nagahama et al. [4]. The weight of scaffolds was measured (W_0), then the degradation buffer was prepared from PBS, pH adjusted to 5.2 with acetic acid, and 0.01 w/v% hen egg white (lysozyme) was added. The samples were immersed in the degradation buffer and incubated at 37°C for 7 and 14 days. After 7 and 14 days, the samples were removed, washed with deionized water, dried and re-weighed W_1. The degradation rate was calculated as following:

$$DR\,(\%) = [(W_0 - W_1)/W_0] \times 100$$

where DR is the biodegradation percentage, W_0 is the weight at zero biodegradation time, and W_1 is the weight after 7 and 14 days, respectively.

2.5 Scanning electron microscope (SEM) studies

The pore structure of the scaffolds was observed on a FEI Quanta 200 scanning electron microscope. The fracture sections of frozen samples were sputter coated with Au prior to observation.

2.6 X-ray diffraction characterization (XRD)

To measure the change of the gallery distance of MMT before and after intercalation, 2D-XRD patterns were recorded with a 0.5° oscillation over 5 min on a Rigaku Micro Max 007 microfocus rotating anode X-ray generator (Cu Kα) with on Axco PX70 capillary optic and a Rigaku RAxis (IV++) image-plate detector. Images were recorded and analyzed with Crystal Clear software (Pflugrath).

2.7 In vitro culture studies

2.7.1 Cell culture

Saos-2 cells were routinely cultured in McCoy's 5A medium supplemented with 15% fetal bovine serum (FBS), while RAW 264.7 cells were grown in RPMI-1640 supplemented with 10% FBS. Both cell lines were incubated at 37°C in humidified air containing 5% CO_2. Media were supplemented with 2 mM L-glutamine, 100 units/ml penicillin G sodium, 100 units/ml streptomycin sulphate, and 250 ng/ml amphotericin B. Monolayer Saos-2 cells were harvested by trypsin/EDTA treatment, while RAW 264.7 cells were collected by gentle scraping.

2.7.2 Preparation of biocomposites for cell treatment

For each cellular experiment, each biocomposite was cut into 5 × 5 mm circles, sterilized by 24 h irradiation using ultraviolet light and then soaked for 24 h to remove excess GA, in sterile distilled water containing 100 units/ml penicillin G sodium, 100 units/ml streptomycin sulphate and 250 ng/ml amphotericin B. A further soaking in PBS containing the same antibiotics for another 24 h was followed by 24 h incubation in McCoy's 5A medium supplemented with 15% FBS. Before assaying, the biocomposites were tested for endotoxin using Pyrogent® Ultra gel clot assay, and they were found endotoxin free. All experiments were repeated four times, unless mentioned, and the data was represented as (mean ± SD).

2.7.3 Saos-2 cells/biocomposites Interaction

Experiments were performed to explore the interaction of different biocomposites with monolayer cells including cell/biocomposite attachment, cell cluster formation and cells viability. Saos-2 cells were stained by acridine orange, a known viable stain for cells. Briefly, Saos-2 cells (5×10^5 cells/dish) were cultured with 10 mg of each prepared biocomposite in Petri-dishes in medium for 16 days. The media were changed every 2 days. The dishes were incubated at 37°C in humidified air containing 5% CO_2. On the last day, the media were discarded and then the cell/biocomposites were covered with 100 μg/ml of acridine orange/PBS and incubated for 30 min at 37°C [27]. Acridine orange was removed and cells were washed several times by PBS. Cells were visualized magnification (×20) using a Zeiss Axioplan2 fluorescence light microscope (Carl Zeiss, Inc., Thornwood, NY). Both laser and low intensity white light to visualize the biocomposite mass and to have enlightened background. Acridine orange stained the viable cells with a green color. Cell clusters were observed and evaluated in each biocomposite. In addition to, the biocomposite degradation in the culture and the cell/biocomposite interactions such as cell morphology, adhesion, penetration and cell growth enrichment in biocomposite were recorded.

2.7.4 Saos-2 cells proliferation

The proliferation of Saos-2 cells was estimated by the 3-(4,5-dimethyl-2-thiazolyl)-2,5-diphenyl-2H-tetrazolium bromide (MTT) assay [28]. Cells were cultured in 6 wells-plates for 24 h in medium (5×10^4 cells/well), and 10 mg of each prepared biocomposite were added to each well ($n = 4$). The plates were incubated at 37°C in humidified air containing 5% CO_2 for different intervals (4, 8 and 16 days), before being submitted to the MTT assay. The

media were changed every 2 days. The absorbance was measured with an ELISA reader (BioRad, München, Germany) at 570 nm. The relative cell viability was determined by the amount of MTT converted to the insoluble formazan precipitate. The data were expressed as the mean percentage of viable cells as compared to the respective control untreated cultures.

2.7.5 Apoptosis and necrosis assay

To screen the effect of the biocomposites on apoptosis and necrosis ratios in Saos-2 cells we used acridine orange/ethidium bromide staining [27]. Saos-2 cells were cultured in four-well plates at a density of 4×10^4 cells/well and treated with 10 mg of each prepared biocomposite for 16 days. The cells were labeled using the nucleic acid-binding dye mix of 100 μg/ml acridine orange and 100 μg/ml ethidium bromide in PBS. The cells were attached to the bottom of the plate, not to the biocomposite, and were examined by fluorescence light microscopy. Viable cells had green fluorescent nuclei with organized structure. The early apoptotic cells had yellow chromatin in the nuclei that were highly condensed or fragmented. Apoptotic cells also exhibited membrane blebbing [29]. The late apoptotic cells had orange chromatin with nuclei that were highly condensed and fragmented. The necrotic cells had bright orange chromatin in round nuclei. Only cells with yellow, condensed, or fragmented nuclei were counted as apoptotic cells in a blind, nonbiased manner [29]. For each sample, at least 500 cells/well and 4 wells/biocomposite were counted, and the percentage of apoptotic cells was determined: % of apoptotic or necrotic cells = (total number of apoptotic or necrotic cells/total number of cells counted) × 100.

2.7.6 Proliferating cell nuclear antigen

For the assessment of proliferating cell nuclear antigen (PCNA), briefly, 20 μg of isolated proteins were applied to PCNA ELISA (# QIA59, Oncogen, MA, USA), which is a sandwich enzyme immunoassay employing a rabbit polyclonal antibody specific for human PCNA protein, a biotinylated mouse monoclonal antibody clone, and horseradish peroxidase-conjugated streptavidin. Saos-2 cells were cultured in 6 wells-plates for 24 h in medium (5×10^5 cells/well), before being treated for 16 days with 10 mg of biocomposites 3, 4 and 7 that were found to induce proliferation, as concluded from MTT assay results. Nuclear lysates were extracted from treated and untreated cells and their protein content was measured by bicinchoninic acid assay [30]. Quantitation of PCNA concentration in samples was achieved by blotting a standard curve of PCNA.

2.7.7 Colorimetric determination of alkaline phosphatase

In order to investigate effects of prepared biocomposite on the alkaline phosphatase activity, Saos-2 cells were plated at a density of 5×10^4 cells/well in serum-free medium containing 0.1% BSA. Cells were incubated at 37°C for 16 days, and then washed with Hanks' balanced salt solution (HBSS). Cell layers were lysed by the addition of 80 ml Triton® X-100 (0.5% in PBS) to each well. A sample of 40 μl of lysate was removed from each well and used to assay alkaline phosphatase activity, and 10 μl were assayed for protein content using the BCA protein assay. Alkaline phosphatase activity was measured as a function of p-nitrophenol hydrolysis from p-nitrophenyl phosphate according to the method of Boyan et al. [31]. Results are expressed as μg alkaline phosphatase/mg cellular protein.

2.7.8 Effect of biocomposites on macrophages proliferation

The effect of different prepared biocomposites on the proliferation of macrophages, as essential immune cells, was assayed by MTT assay [28]. RAW macrophage 264.7 was cultured in 6 wells-plates for 24 h in medium (5×10^5 cells/well) and 10 mg of each prepared biocomposite were added to each well ($n = 4$). The plates were incubated at 37°C in humidified air containing 5% CO_2 for 4 days, before being submitted to MTT assay. The data were expressed as the mean percentage of viable cells as compared to the control untreated cultures.

2.7.9 Inflammatory effect of biocomposites

The accumulation of nitrite, an indicator of NO synthesis, was measured by Griess reagent [32]. RAW 264.7 were grown in phenol red-free RPMI-1640 containing 10% FBS in 6 wells-plate. Macrophages were incubated for 4 days with 500 ng/ml of bacterial lipopolysaccharide (LPS) or biocomposites (10 mg/well). A non-isoform-specific NO synthase inhibitor, NG-monomethyl-L-arginine (L-NMMA) at 250 μM was used as a reference inhibitor of NO production instead of biocomposites. 50 μl of cell culture supernatant were mixed with 50 μl of Griess reagent and incubated for 10 min. The absorbance was measured spectrophotometrically at 550 nm. A standard curve was blotted using serial concentrations of sodium nitrite. The nitrite content was normalized to the cellular protein content as measured by bicinchoninic acid assay.

2.8 Statistical analysis

MTT assay data were analyzed by using two-factorial analysis of variance (ANOVA), including first-order

interactions (two-way ANOVA), followed by the Tukey post hoc test for multiple comparisons. Other test data were analyzed by using one-way ANOVA followed by the Tukey post hoc test. $P < 0.05$ indicated statistical significance.

3 Results and discussion

3.1 Effect of biocomposite composition on the swelling behavior

The water adsorption content is an important index to the scaffolds [33, 34], in other words, an important property which is related to the pore size, the interconnection conditions, and the scaffold volume. Substantial changes in S_w (%) were noted at different pH values (2.0, 7.4 and 9.0) depending on MMT and Cel concentrations, in addition to the type of crosslinker (GA and MBA) as shown in Fig. 1a–d.

The solid concentration of G-MMT/Cel scaffold solution and the crosslinker types (GA and MBA) crucially influence pore size and porosity, consequently affecting the swelling behavior. Generally, when the concentration of GA was increased, the swelling was decreased as shown in Fig. 1a. At high pH values (pH 9.0), the swelling behavior showed a significant increase relative to that at lower values. This may be due to the negative charge repulsive forces between Gel chains being increased which resulted in an increase in the swelling of the scaffold. On the other hand, the crosslinked Gel has an isoelectric pH (IP) in the range of 4.7–5.1. Below the IP value, the Gel chains remain protonated. As a result, the chains contain (NH_3^+) ions, and the cationic repulsion between them could be responsible for their high swelling [35]. The mechanism of GA crosslinking is complex, involving many possible reactions [36], primarily with amino groups as follows: a) both aldehyde groups form a Schiff base with the ε-amino groups of lysine to form a dipyridine structure [37]; b) only one of the aldehyde groups reacts with an amino group

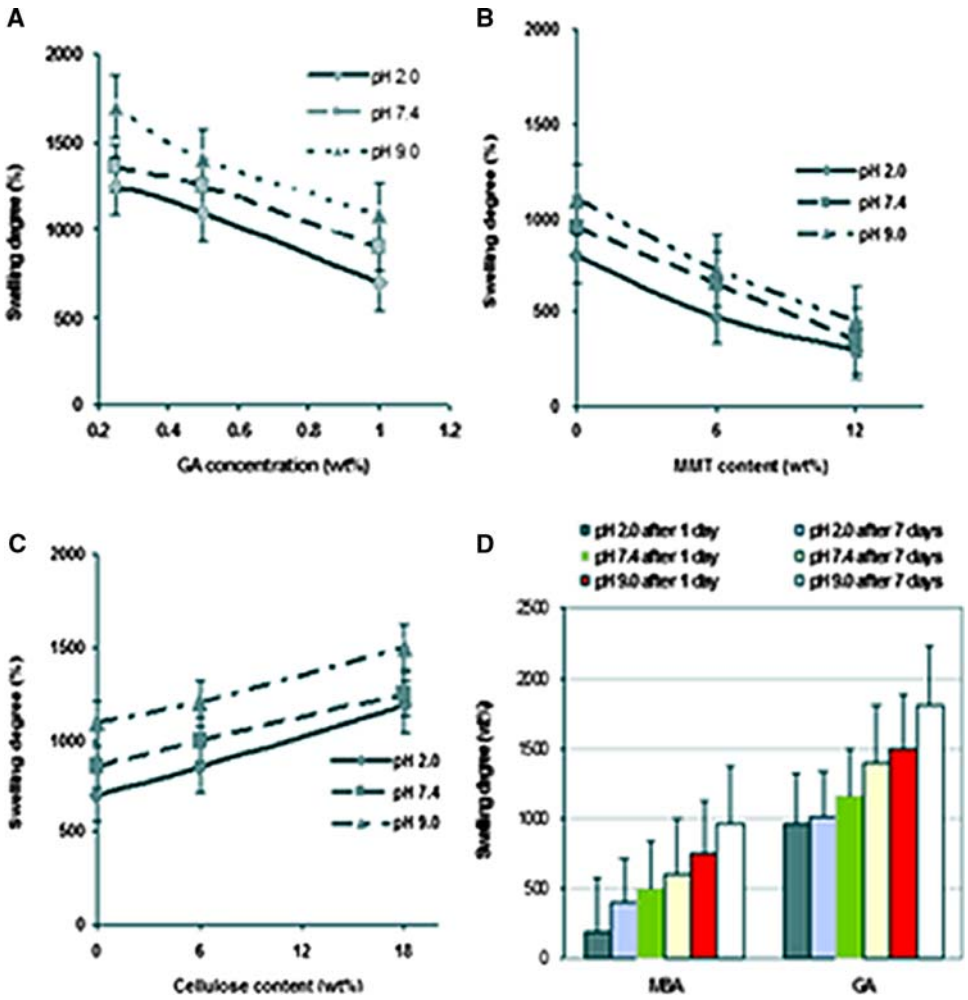

Fig. 1 Effect of **a** GA (in case of samples 2, 3 and 4), **b** MMT (in case of samples 3, 5 and 6), **c** cellulose (in case of samples 6, 7 and 8) and **d** different crosslinking agents (GA and MBA, in case of samples 1 and 3, respectively) on water absorption content of the scaffolds after soaking in PBS for 7 days at different pH (2.0, 7.4 and 9.0)

leaving the other one unreacted; c) GA might be grafted into more complex polymers; and d) GA forms polymers through an aldol condensation reaction. In addition it is known that GA crosslinks formed as Schiff bases are unstable, reversible, and long-range crosslinks may depolymerize overtime. The effect of MMT microparticles on the water adsorption content is shown in Fig. 1b. The water adsorption content decreases when increasing the MMT amount in different pH media and different period of times. Because of the barrier effect of microsized sheets of MMT, the interaction between Gelatin–Cellulose macromolecules and water molecules is inhibited, which results in the drop of the water content values. Cellulose has many hydrophilic hydroxyl groups, consequently, the biocomposites which have high cellulose content exhibited higher swelling degrees relative to that have low content (Fig. 1c). From Fig. 1d, as expected, it can be observed that, the swelling degree of the crosslinked biocomposites was increased with increasing both the pH and the time of soaking in the buffer media. In general, the crosslinked biocomposites using GA have higher swelling than that in case of using MBA, which may be due to high crosslinking efficiency of MBA in comparison with GA.

3.2 In vitro degradation behavior

As the tissue engineering aims at regeneration of new tissues, the scaffolds are expected to be degradable and absorbable with a proper rate to match the speed of new tissues formation. The degradation behavior of biomaterials in physiological environments plays an important role in the engineering process of a new tissue. In our work, the in vitro biodegradation of Gel–MMT/Cel biocomposites in PBS containing lysozyme was investigated. The results are illustrated in Fig. 2a–c. The degradation process involves Gel hydrolysis.

From Fig. 2b, it was observed that, crosslinked Gel degrades faster at low GA concentration in comparison with high concentration one. This may be due to the large quantity of hydrophilic amino and carboxyl groups at lower degree of crosslinking. The effect of MMT content on the degradation behavior is shown in Fig. 2c. As it is revealed, the degradation percentage dramatically decreases with increasing the MMT content. It is reasonable to think that the strong interaction between gelatin macromolecular chains and MMT sheets consumes some hydrophilic groups and depresses the solvent uptake, which protects the macromolecules from hydrolyzing. Meanwhile, the presence of MMT also provides physical crosslinking sites, which enhance the stability of the network. It can be concluded that the degradation rate may be controllable by adjusting the MMT content.

3.3 XRD characterization of Gel–MMT/Cel biocomposites

Amorphous Gel cast above 35°C undergoes a major glass transformation in the region 125–200°C according to the preparation conditions. On the other hand, semi-crystalline Cel has many hydroxyl groups. Polyelectrolyte complexes can be formed by the reaction of oppositely charged polyelectrolytes in an aqueous solution. According to previous work [38], hydrophilic Gel chains can be inserted into MMT layers via the solution intercalation process. Gel–MMT hybrid material was directly prepared with unmodified MMT and Gel aqueous solution as in previous work [39], and an intercalated or partially exfoliated structure was achieved. This intercalation allows for the insertion of hydrophilic Gel chains into the MMT layers. When the concentration of Gel solution exceeded 10%, it was difficult to intercalate. The distances between MMT layers were gradually increased with increased reaction temperature (60–80°C) and a better intercalation effect is achieved. XRD-patterns of Gel–Cel biocomposite change dramatically in comparison with Gel–MMT, as shown in Fig. 3a and Table 1. Some of the diffraction peaks of G–MMT and MMT shift towards lower angle values and some of these become broad and even disappear in comparison with G–MMT–Cel indicating that intercalation structure have been formed. The interlayer spacing increases from 15.8 to 17.55 A°, and 18.0 A° due to the insertion of gelatin molecules into the sheets of MMT.

3.4 Microstructure of Gel–MMT/Cel biocomposites

The proper microstructure of pores is the key point to exert the scaffold efficacy, which includes the pore size, porosity, inter-connection between the pores, and surface/volume ratio. The scaffold porosity should be high enough and permeable enough to facilitate the in growth of blood vessels, the transportation of nutrients and the removal of waste products, so that the survival of the transplanted cells is ensured. SEM observation of the Gel–MMT–Cel composite scaffolds shows a continuous structure of well-interconnected pores that is similar to the Gel–Cel scaffold (Fig. 3b). The pores size of G–MMT–Cel scaffolds with 6 wt% MMT is around 300 μm. When the MMT content increased to 12 wt%, the pore shape becomes irregular with a lower interconnection degree. It is possible that MMT particles with higher surface energy will aggregate in the solution when the MMT content is high enough.

3.5 Interaction of Saos-2 cells with biocomposites

The interaction of different types of prepared biocomposites with the monolayer Saos-2 cells including cell/

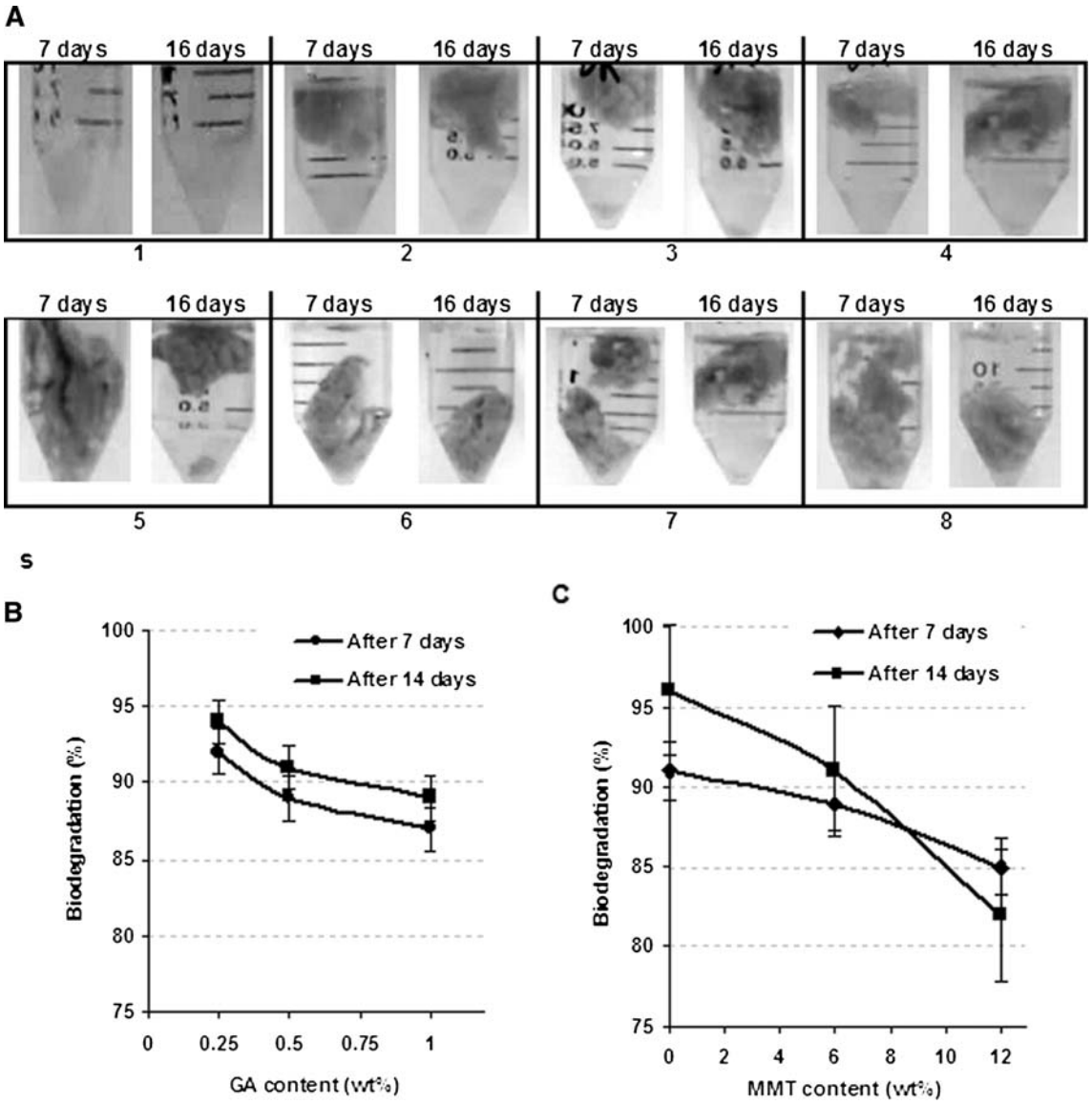

Fig. 2 **a** Photos of In vitro biodegradation of the prepared scaffolds; after 7 and 14 days, Effect of **b** GA (in case of samples 2, 3 and 4) and **c** MMT content (in case of samples 3, 5 and 6) on the in vitro biodegradation of the scaffolds

biocomposite attachment, penetration, cluster formation and vitality of cells was investigated in Saos-2 cells using acridine orange, which stained the vital cells a green fluorescent color. Cells were seeded with different types of biocomposites and visualized and analyzed by fluorescence microscope, in presence of low intensity white light.

After seeding of Saos-2 cells for 16 days with biocomposites 1, 2 and 4, the staining with acridine orange revealed that none of these biocomposites had Saos-2 cells attached on the surface, nor had cells penetrated into the interior pores of any biocomposite (Fig. 4) and consequently no cell clusters were found (Table 2). It is observed also that the matrix of the biocomposites 1, 2 and 4 was stiff, not degraded, and not fragmented in the presence of cells and cell culture medium for 16 days. On the other hand, we observed that there was a remarkably low affinity of attachment (only to the margins), and penetration of Saos-2 cells when seeded with biocomposites 3 and 7 (Fig. 4). No cell clusters could be counted on biocomposite 3, due to the low number of attached cells (Fig. 4 and Table 2), while less than 25 cell clusters were counted on the margin surface of biocomposite 7 (Table 2). It was also noticed that the matrix of biocomposite 3 loss the stiffness and was fragmented into fiber-like fragments in the presence of cells and cell culture medium for 16 days. Alternately, the seeding of biocomposite 5 with Saos-2 cells revealed a relatively high cell attachment (Fig. 4) and cluster formation. It is also observed that, after 16 days,

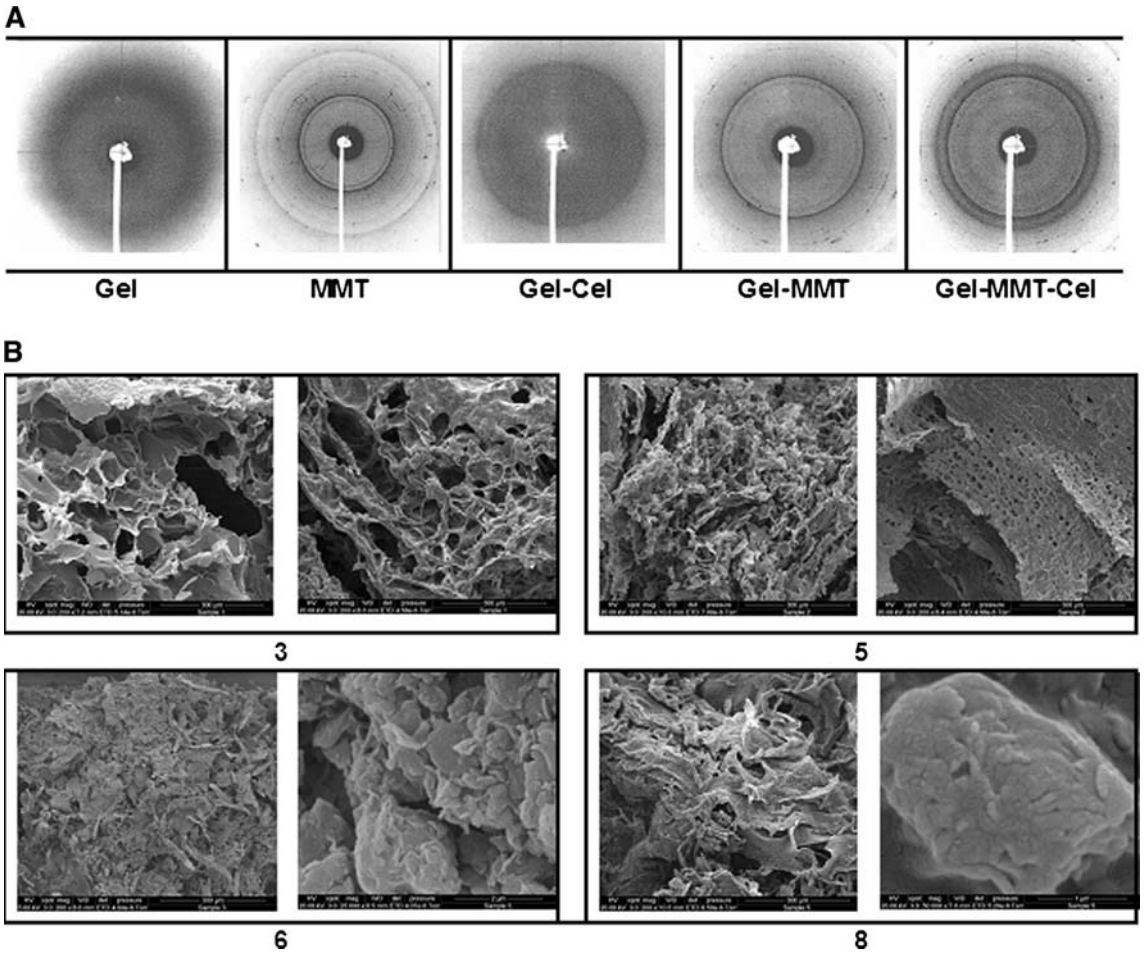

Fig. 3 **a** 2D-XRD diffraction patterns of scaffolds; at G:Cel = 1:1; 6% MMT; and 0.5% GA, **b** SEM-Micrographs of the scaffolds 3, 5, 6 and 7

Table 1 2D-XRD data of the prepared biocomposites

Sample code	d (A°)	XRD-description
Gel	4.6	Amorphous
MMT	2.55, 2.99, 3.85, 4.42, 4.9, 10.3, 15.8	Disordered semicrystalline
8	2.56, 2.86, 3.71, 4.43, 4.92, 9.7, 17.55	Semicrystalline
3	3.94, 4.43, 5.6	Semicrystalline
5	3.86, 4.46, 4.92, 6.0, 10.2, 18.0	Semicrystalline

although the matrix of biocomposite 5 had not fragmented, it was highly degraded in the cell culture media. From the photographs (Fig. 4), it is can be clearly seen that Saos-2 cells were able to split, migrate, adhere and proliferate on the surface, and in the interstitial layer of the seeded biocomposites 6 and 8 showing that they are effective cell scaffolds. Cells of fusiform shape were observed to firmly attach on the scaffold wall, spread well and grow into the interior parts of the scaffolds to form in vitro cell/scaffold constructs (Fig. 4). Within 16 days, besides the evident growth and attachment of the cells onto the porous scaffold, the outside layer surface of scaffold was fully covered by confluent cells, indicating that there were no direct toxic effects and cellular metabolism was normal. The cells effectively colonized the porous structure of the scaffolds 6 and 8 and the cell clusters were counted at greater than 100 clusters (Table 2). It is also noticed that the matrix of biocomposite 6 and 8 was fragmented into small pieces (Fig. 4), highly degradable and they were all covered with cells after seeding in the culture media environment for 16 days. From these findings, it is clear that the absence of MMT lead to poor or no cell adhesion

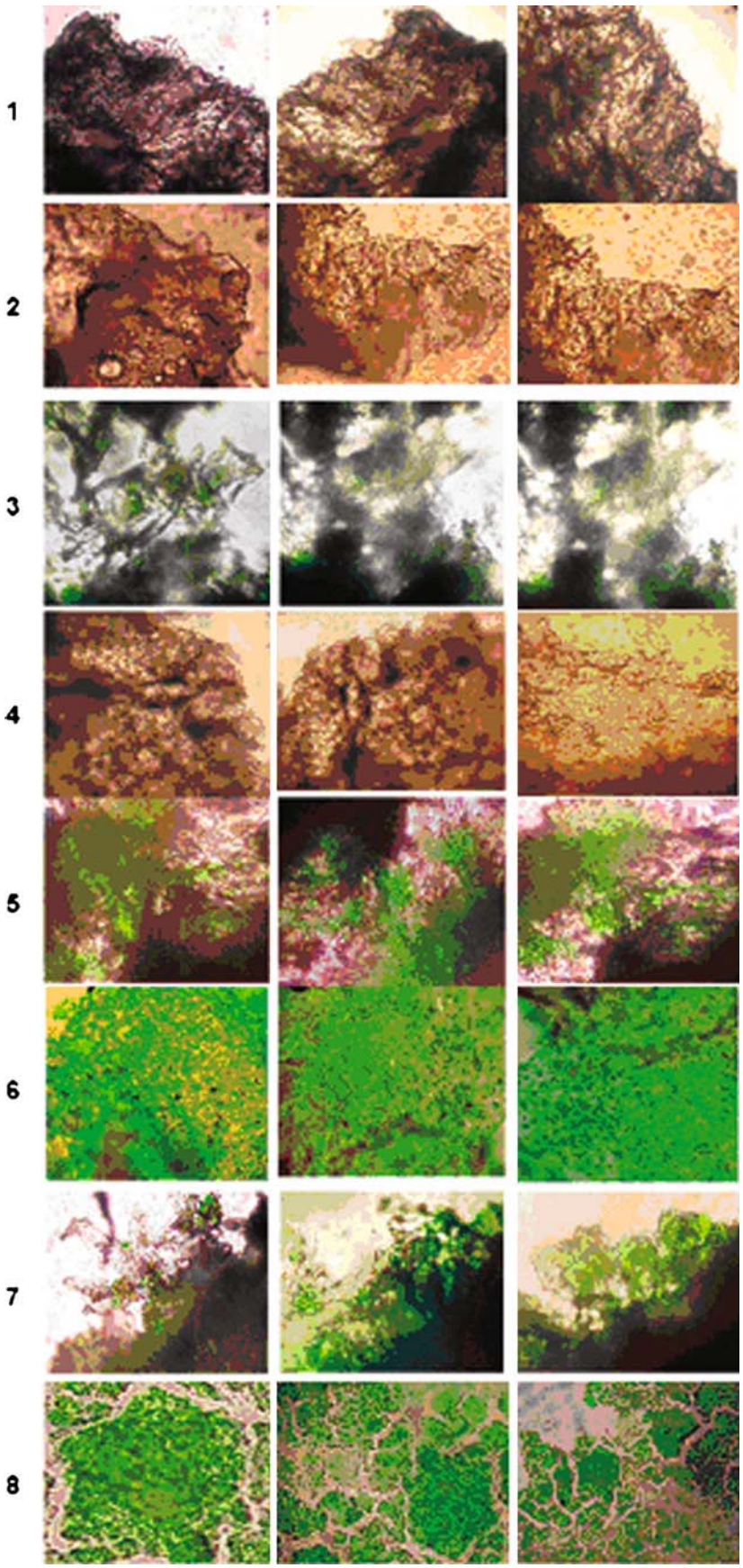

Fig. 4 Photographs for the interactions between different biocomposites (1–8) and Saos-2 cells. Cells were stained with acridine orange (*vital cells are in green color*), and they were visualized by fluorescence microscope (×400). Cells were treated with 10 mg of each biocomposite for 16 days

Table 2 The composition of different prepared biocomposites (1–8) and the results of Saos-2 cells/biocomposite interactions after 16 days of co-culture, as conducted from fluorescence microscope observation after staining with acridine orange

	Biocomposites							
	1	2	3	4	5	6	7	8
1. Biocomposites composition								
Gel	6%	6%	6%	6%	6%	6%	6%	6%
Cel	6%	6%	6%	6%	6%	6%	18%	–
MMT	–	–	–	–	6%	12%	6%	6%
GA	–	0.2%	0.5%	1%	0.5%	0.5%	0.5%	0.5%
MBA	0.5%	–	–	–	–	–	–	–
2. Cell/Biocomposite interaction								
Cell attachment	−	−	+	−	+	+	+	+
Formation of cell clusters	−	−	−	−	+	+	+	+
Number of cell clusters	−	−	−	−	<50	>100	<25	>100

and consequently no cell penetration and cluster formation as found in the case of biocomposites 1, 2, 3, and 4. The cross linking by 0.5% MBA, instead of GA, did not change that improve on this situation (Table 2). Moreover, results indicated that the increase of the cellulose content in the biocomposite 7 diminished the adhesion, penetration and cluster formation of Saos-2 cells, compared with biocomposite 5. The increase of MMT content in the biocomposite 6 dramatically improved adhesion, penetration and cluster formation of the cells, compared with biocomposite 5. Surprisingly, the total absence of cellulose from the biocomposite 8 did not negatively affect the cellular functions but in contrast it led to remarkably enhanced adhesion, penetration and cluster formation of Saos-2 cells. It is known that cell adhesion is an important cellular process that directly influences the further proliferation and tissue formation. Biocomposites 6 (6% Gel/6% Cel/12% MMT cross linked by 5% GA) and 8 (6% Gel/6% MMT cross linked by 0.5% GA) seem to be the most efficient and effective biodegradable scaffolds for cell adhesion, penetration, and cluster formation in cell culture.

3.6 Effect of scaffolds on the proliferation of Saos-2 cells

The biocompatibility of different prepared biocomposites was preliminary investigated via studying the metabolic vitality of Saos-2 by MTT assay, which assessed the mitochondrial redox activity. The yellow tetrazolium salt of MTT is reduced by mitochondrial enzyme succinate dehydrogenase, present in living cells, to form insoluble purple formazan crystals, which are solubilized by the addition of a detergent.

As Fig. 5a shows seeding of Saos-2 cells with biocomposites 1, 2, 3 and 7 for different intervals (4, 8 and 16 days) led to a noticeable time-dependant inhibition of cell proliferation. Biocomposite 3 was the most significant growth inhibitor ($P < 0.05$), especially after 8 and 16 days of incubation. Additionally, co-culture of cells with biocomposites 4 and 5 exhibited insignificant change in the cell growth. On the other hand, seeding of Saos-2 cells with biocomposites 6 and 8 resulted in a significant induction in the cell proliferation ($P < 0.05$), starting from the 4 days to 16 days of incubation. Taken together from those finding it can be concluded that biocomposites 1, 2 and 3 were cytotoxic to Saos-2 cells and that biocomposites 6 and 8 were promising for Saos-2 cells proliferation.

3.7 Assessment of apoptosis and necrosis

To screen the effect of biocomposites 1, 2, 3 and 4, which showed growth inhibition and cytotoxicity, on the apoptosis and necrosis in Saos-2 cells, we used acridine orange/ethidium bromide staining. The percentage of apoptotic and necrotic cells was determined to evaluate the extent of death of the cells. The staining identified multiple cells undergoing apoptosis after being seeded with biocomposites 1 and 3, but 3 was the highest apoptosis inducer, while biocomposite 2 was the highest inducer of necrosis in Saos-2 cells (Fig. 5b). This may be due to the high percentage of GA (0.5%) relative to that in case of biocomposite 1 (0.25%). As expected, the residual uncrosslinked GA released from the biocomposite 3 after soaking period of 4, 8 and 16 days [40] and consequently the cytotoxicity was increased and the viable cells were reached the minimum value at that time. Moreover, the cells were attached to the bottom of the plate not to the biocomposites and the apoptotic cells are in the nuclei which are highly condensed and fragmented. While necrotic cells are in the round nuclei at early stage of Saos-2 cell culture in the presence of the biocomposites.

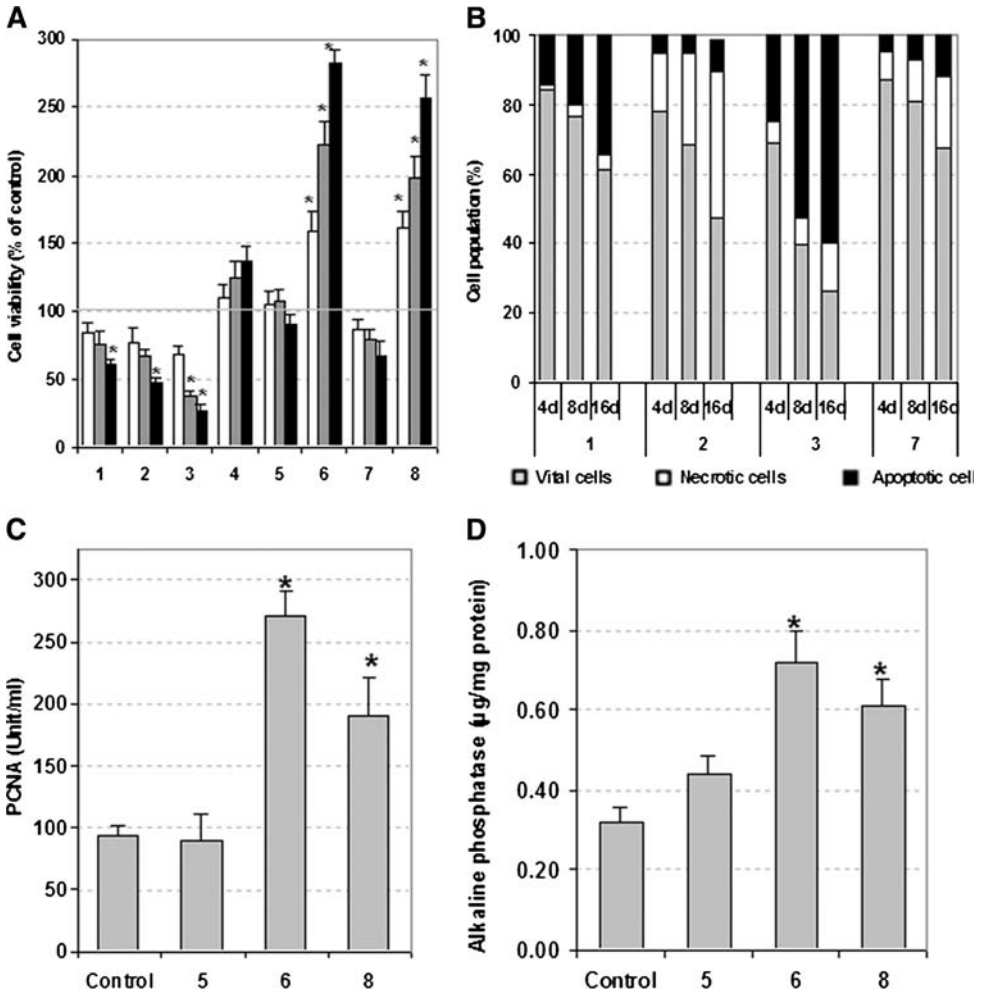

Fig. 5 **a** The effect of the incubation with different biocomposites (10 mg/ml) for variable intervals 4 days (*white bars*), 8 days (*gray bars*), and 16 days (*black bars*) on the proliferation rate of Saos-2 cells, was estimated by MTT assay. The change in Saos-2 cells proliferation rate was expressed as percentage of control untreated cells (Mean ± SD, $n = 3$). **b** The type of death in Saos-2 cells after being seeded with 10 mg/ml of cytotoxic biocomposites 1, 2, 3, and 7 for 16 days, was estimated by staining with acridine orange/ethedium bromide. The stained cells were visualized under fluorescence microscope (×400) and the percentage of apoptotic (*black segments*), necrotic (*white segment*) and vital (*gray segments*) cells were counted. **c** Evaluation of PCNA level in the lysate of Saos-2 cells was assayed by ELISA, after incubation with 10 mg/ml biocomposites 5, 6 and 8 for 16 days. The data are expressed as unit/ml (Mean ± SD, $n = 3$). **d** The effect of the co-incubation of Saos-2 cells with 10 mg/ml biocomposites 5, 6 and 8 for 16 days, on the alkaline phosphatase level, was estimated by colorimetric assay. The alkaline phosphatase content in differentiated was expressed as µg/mg protein (Mean ± SD, $n = 3$)

3.8 Evaluation of proliferating cell nuclear antigen

To explore the factors that lead to the enhanced proliferation, to variable extents, in Saos-2 cells after co-cultured with biocomposites 5, 6 and 8, we measured PCNA in the cells. PCNA is essential in many pathways including: cell cycle control, DNA replication, nucleotide excision repair, and post replication mismatch repair [41]. PCNA is a marker for cells in early G1 phase and S phase of the cell cycle. It is found in the nucleus and it is a cofactor of DNA polymerase delta, it acts as a homotrimer and helps increase the processivity of leading strand synthesis during DNA replication [40]. Our results indicated that biocomposite 5 did not significantly change the PCNA expression, while biocomposites 6 and 8 led to significant elevation in PCNA in comparison with the untreated cells (Fig. 5c). These findings may explain the dramatic enhancement in the cell proliferation with biocomposites 6 and 8 due to the induced PCNA and accordingly the DNA synthesis.

3.9 Determination of alkaline phosphatase

Osteogenic lineages express alkaline phosphatase, a polyfunctional enzyme which plays an important role bone formation, in mineralization and can bind Ca^{2+}, transport

inorganic phosphate and regulate cell division [42]. The differential function of the cells was assessed by testing their alkaline phosphatase activity. In order to investigate effects of the promising biocomposites 5, 6 and 8 on the alkaline phosphatase activity, Saos-2 cells were incubated for 16 days with each. Our results indicated that biocomposite 5 led to insignificant elevation of alkaline phosphatase activity; however biocomposites 6 and 8 resulted in a significant increase in the activity of the enzyme (Fig. 5d). These findings provide a promising application for biocomposites 6 and 8 in tissue engineering of bones as bone scaffolds through enhancing of bone regeneration and formation.

3.10 Effect of biocomposites on the proliferation of macrophages

We investigated the effect of different biocomposites on the proliferation of macrophages, as essential immune cells in the innate immunity that defend the cells against no-self materials. RAW macrophage 264.7 was treated for 4 days with each biocomposite and then assayed by MTT assay. The experiment indicated that biocomposites 4, 5, 6 and 8 had non-significant effect of macrophage growth, while biocomposites 1, 2, 3 and 7 dramatically inhibited the macrophage growth but to different extents (Fig. 6a). Similarly as in case of Saos-2 cells biocomposite 3 was the most cytotoxic against macrophages. This may be due to the biocomposite 7, which has high cellulose content (18%), diminished the adhesion, penetration and cluster formation of Saos-2 cells.

3.11 Inflammatory effect of biocomposites

Macrophages when stimulated by non-self agent or pathogen, secrete many inflammatory mediators. NO is one of the key mediators in the inflammation process. The accumulation of nitrite, an indicator of NO synthesis, was measured cell culture media. RAW 264.7 were incubated for 4 days with LPS or non cytotoxic biocomposites 5, 6 and 8. All the tested biocomposites exhibited no effect on the nitrite level compared to the highly induced nitrites after treatment of macrophage with LPS (Fig. 6b). These results represent a preliminary experiment on the negative immunoreactivity and inflammatory effect of all of those biocomposites, especially the promising scaffolds 6 and 8.

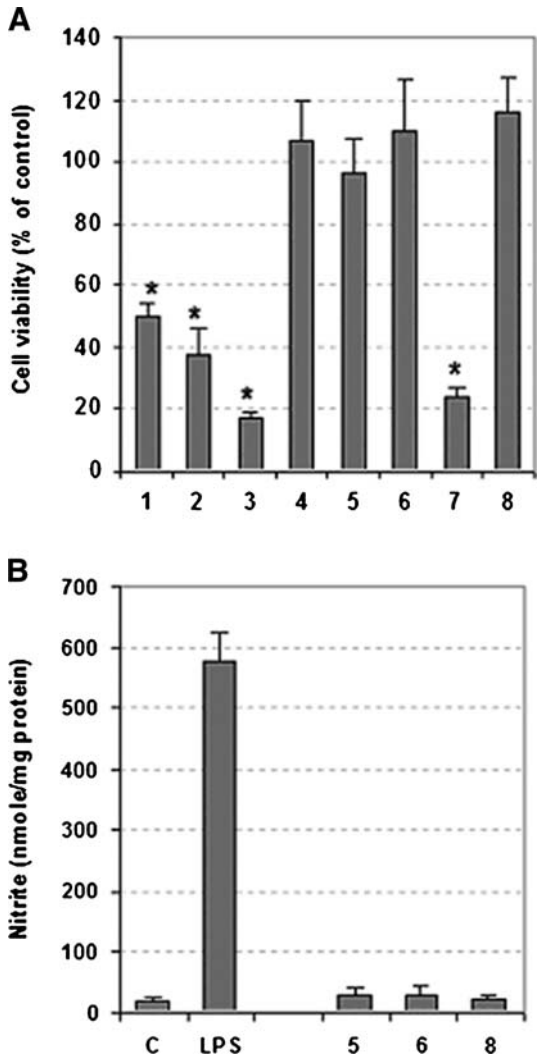

Fig. 6 **a** The effect of the incubation with different biocomposites (10 mg/ml) for 4 days (on the proliferation of RAW macrophage 264.7 cells, was estimated by MTT assay. The change in the macrophages proliferation rate was expressed as percentage of control untreated cells (Mean ± SD, $n = 3$). **b** The inflammatory effect of the promising biocomposites 5, 6, and 8 (10 mg/ml) was assayed by evaluating the nitrites content (as an index for NO generation, inflammatory mediator) in the macrophage supernatants, using Griess assay, after 4 days of incubation with the biocomposites. The data was expressed as nmole nitrites/mg protein

4 Conclusions

The Gel–MMT/Cel biocomposite scaffolds prepared by the freeze-drying possessed suitable pore structure to be used as a biomimetic substrate for tissue engineering. The incorporation of small amount of MMT microsheets may be used to tailor the structural stiffness to fit the requirements of a board range of soft scaffolds applications. Data reveal that the in vitro degradation rate is greatly affected by the incorporation of MMT, and it may be a controllable effect when adjusting the MMT contents. The successful generation of 3-D biomimetic structures incorporating from Saos-2 cells indicates their potential for de novo bone formation that exploits cell–matrix interactions. In vitro studies revealed that the scaffolds (6% Gel/6% Cel/12% MMT cross linked by 5% GA) and (6% Gel/6% MMT

cross linked by 0.5% GA) seem to be the most efficient and effective of the biodegradable scaffolds studied. They promoted the cell proliferation, migration, expansion, adhesion, penetration, spreading, and differentiation of human osteosarcoma cells (Saos-2) on these 3-D scaffolds. MMT improved cytocompatibility between the osteoblasts and the biocomposite. In vitro analysis indicates good biocompatibility of the scaffold as a new potential candidate as biohybrid material for tissue engineering. The advantage of these novel scaffolds compared to other ones already reported in the literature is that the lower rate of biodegradation in the physiological fluids which leads to an accurate simulation of the degradation profile in vivo that would be difficult since the numerous types and concentrations of hydrolytic enzymes involved in the process.

Acknowledgements Dr. A. A. Haroun would like to thank laboratories of Prof. D. R. K. Harding and Prof. G. Jameson at College of Sciences, Palmerston North, Massey University, New Zealand for support and generous assistance toward carrying out some of the necessary investigations in this work, during his scientific visit. Also, this work was supported by Center of Excellence for Advanced Sciences, National, Research Center, Cairo, Egypt.

References

1. Zheng JP, Wang CZ, Yao KD. Preparation of biomimetic three-dimensional gelatin/montmorillonite-chitosan scaffold for tissue engineering. React Funct Polym. 2007;67:780–8.
2. Dasdia T, Bazzaco L, Dolfine E. Organ culture in 3-dimensional matrix. In vitro model for evaluating biological compliance of synthetic meshes for abdominal wall repair. J Biomed Mater Res. 1998;43:204–9.
3. Grande DA, Halberstadt C, Manji R. Evaluation of matrix scaffolds for tissue engineering of articular cartilage grafts. J Biomed Mater Res. 1997;34:211–20.
4. Nagahama H, Kashiki T, Tamura H. Preparation of biodegradable chitin/gelatin membranes with GlcNAc for tissue engineering applications. Carbohydrate Polymers 2008; online, http://www.sciencedirect.com.
5. Lee SB, Kim YH, Lee YM. Study of gelatin-containing artificial skin V: fabrication of gelatin scaffolds using a salt-leaching method. Biomaterials. 2005;26:1961–8.
6. Muzzarelli RA. Biochemical significance of exopenous chitins and chitosans in animals and patients. Carbohydr Polym. 1993;20:7.
7. Choi YS, Hong SR, Nam YS. Study on gelatin-containing artificial skin I: preparation and characteristics of novel gelatin-alginate sponge. Biomaterials. 1999;20:409–17.
8. Martucci JF, Ruseckaite RA, Vazquez A. Creep of glutaraldehyde-crosslinked gelatin films. Mater Sci Eng A. 2006;435:681–6.
9. Achet D, He XW. Determination of the renaturation level in gelatin films. Polymer. 1995;36:787–91.
10. Arvanitoyannis IS, Nakayama A, Aiba S. Chitosan and gelatin based edible films: state diagrams, mechanical and permeation properties. Carbohydr Polym. 1998;37:371–82.
11. Awad H, Erickson G, Guilak F. Biomaterials for cartilage tissue engineering. In: Lewandrowski KU, Wise D, Trantolo D, Gresser J, Yaszemski M, Altobelli D, editors. Tissue engineering and biodegradable equivalents: scientific and clinical applications. New York: Marcel Dekker Inc; 2002. p. 267–99.
12. Xia W, Lu W, Cao Y. Tissue engineering of cartilage with the use of chitosan–gelatin complex scaffolds. J Biomed Mater Res Part B: Appl Biomater. 2004;71B:373–80.
13. Huang Y, Onyeri S, Madihally SV. In vitro characterization of chitosan–gelatin scaffolds for tissue engineering. Biomaterials. 2005;26:7616–27.
14. Couderc H, Delbreilh L, Saiter JM. Relaxation in poly(ethylene terphthalate glycol)/montmorillonite nanocomposites studied by dielectric methods. J Non-Cryst Solids. 2007;353:4334–8.
15. Zheng JP, Li P, Yao KD. Preparation and characterization of gelatin/montmorillonite nanocomposite. J Mater Sci Lett. 2002;21:779–81.
16. Ito M, Nagai K. Evaluation of degradation on nylon-6 and nylon-6/montmorillonite nanocomposite by color measurement. J Appl Polym Sci. 2008;108:3487–94.
17. Fan J, Chen G, Zongneng QI. SEM study of a polystyrene/clay nanocomposite. J Appl Polym Sci. 2002;83:66–9.
18. Kawasumi M, Hasegawa N, Okada A. Preparation and mechanical properties of polypropylene-clay hybrids. Macromolecules. 1997;30:6333–8.
19. Agag T, Koga T, Takeichi T. Studies on thermal and mechanical properties of polyimide-clay nanocomposites. Polymer. 2001;42:3399–408.
20. Gang Z, Kun F, Pingsheng H. Study on bulk intercalation polymerization of PMMA/montmorillonite intercalated nanocomposite by dynamic torsional vibration method. J Mater Sci Lett. 2002;21:761–3.
21. Kojima Y, Usuki A, Kamigaito O. Mechanical properties of nylon 6-clay hybrid. J Mater Res. 1993;8:1185.
22. John MJ, Thomas S. Biofibers and biocomposites review. Carbohydr Polym. 2008;71:343–64.
23. Czaja KW, David J, Brown RM. The future prospects of microbial cellulose in biomedical applications review. Biomacromolecules. 2007;8:1–12.
24. Coradin T, Bah S, Livage J. Gelatin/silicate interactions: from nanoparticles to composite gels. J Colloids Surf B: Biointerfaces. 2004;35:53–8.
25. Chao GT, Qian ZY, Wei YQ. Synthesis, characterization, and hydrolytic degradation behavior of a novel biodegradable pH-sensitive hydrogel based on polycaprolactone, methacrylic acid and poly(ethylene glycol). J Biomed Mater Res Part A. 2008;85:36–46.
26. Kenawy E, El-Newehy M, Ottenbrite RM. A new degradable hydroxamate linkage for pH-controlled drug delivery. Biomacromolecules. 2007;8:196–201.
27. Giuliano M, Lauricella M, Tesoriere EG. Induction of apoptosis in human retinoblastoma cells by topoisomerase inhibitors invest ophthalmol. Vis Sci. 1998;39:1300–11.
28. Hansen MB, Nielsen SE, Berg K. Re-examination and further development of a precise and rapid dye method for measuring cell growth/cell kill. J Immunol Methods. 1989;119:203.
29. Gohel A, Mccarthy M, Gronowicz G. Estrogen prevents glucocorticoid-induced apoptosis in osteoblasts in vivo and in vitro. Endocrinology. 1999;140:5339–47.
30. Smith PK, Krohn R, Klenk DC. Measurement of protein using bicinchoninic acid. Anal Biochem. 1985;150:76–80.
31. Boyan BD, Schwartz Z, Swain LD. Localization of 1, 25-(OH)2D3-responsive alkaline phosphatase in osteoblast-like cells and growth cartilage cells in culture. J Biol Chem. 1989;264:11879–86.
32. Gerhäuser C, Klimo K, Frank N. Mechanism-based in vitro screening of potential cancer chemopreventive agents. Mutat Res. 2003;523:163–72.

33. Mikos AG, Lyman MD, Langer R. Wetting of poly(L-lactic acid) and poly(DL-lactic-co-glycolic acid) foams for tissue culture. Biomaterials. 1994;15:55–8.
34. Gao J, Niklason L, Langer R. Surface hydrolysis of poly(glycolic acid) meshes increases the seeding density of vascular smooth muscle cells. J Biomed Mater Res. 1998;42:417–24.
35. Burugapalli K, Bhatia D, Choudhary V. Interpenetrating polymer networks based on poly(acrylic acid) and gelatin. I: swelling and thermal behaviour. J Appl Polym Sci. 2001;82:217–27.
36. Nickerson MT, Paulson AT, Rousseau D. Some physical properties of crosslinked gelatin-moltdextrin hydrogels. Food Hydrocolloid. 2007;20:1072–9.
37. Matsuda S, Iwata H, Ikada Y. Bioadhesion of gelatin films crosslinked with glutaraldehyde. J Biomed Mater Res. 1999;45:20–7.
38. Zheng JP, Xi LF, Yao KD. Correlation between reaction environment and intercalation effect in the synthesis of gelatin-montmorillonite hybrid nanocomposite. J Mater Sci Lett. 2003;22:1179–81.
39. Zheng JP, Li P, Yao KD. Preparation and characterization of gelatin-montmorillonite nanocomposite. J Mater Sci Lett. 2002;21:770–81.
40. Lin FH, Yao CH, Sun JS, Liu HC, Huang CW. Biological effects and cytotoxicity of the composite composed by tricalcium phosphate and glutaraldehyde crosslinked gelatin. Biomaterials. 1998;19:905–17.
41. Jonsson ZO. Proliferating cell nuclear antigen: more than a clamp for DNA polymerases. Bioassay. 1997;19:967–75.
42. Kamali N, McCulloch G, Limeback H. Direct flow cytometric quantification of alkaline phosphatase activity in rat bone marrow stromal cells. Hisrochem Cytochem. 1992;40:1059–65.